PROCEEDINGS OF SCIENCE

Simulation study on cosmic ray shower rate variations with LHAASO-KM2A during thunderstorms

Ci Yang,* Xunxiu Zhou, Xuejian Chen and Daihui Huang (on behalf of the LHAASO Collaboration)

School of Physical Science and Technology, Southwest Jiaotong University, Chengdu 610031, China

E-mail: hdhamy@sina.com

Abstract: The Large High Altitude Air Shower Observatory (LHAASO) has three sub-arrays, KM2A, WCDA, and WFCTA. As the major array of LHAASO, KM2A has been operating stably in shower mode. To study the near-earth atmospheric electric field (AEF) effect on the trigger event rate during thunderstorms, Monte Carlo simulations are performed with CORSIKA and G4KM2A. According to the simulations, the shower rate variations are found to be strongly dependent on the strength and polarity of the AEF. The shower rates increase with the field intensity. In positive AEF (defined as the direction pointing towards the ground), the increased amplitude is less than that in negative AEF. With the same field strength 1000 V/cm, the value exceeds 12% in a negative field, and merely is up to 6% in the positive one. The dependence of the trigger rate variation on the thickness of the AEF layer is also simulated. The shower event rate increases dramatically at small thickness, and then the trend of variation slows down with the AEF layer thickness. This indicates that the AEF with larger layer thickness has more deflection effects on the development of an extensive air shower. The shower rate variations are also found to be dependent on the primary zenith angle. Our simulation results could be useful in understanding the variation of trigger rate detected by LHAASO-KM2A during thunderstorms.

Keywords: Thunderstorms, Cosmic rays, LHAASO-KM2A

38th International Cosmic Ray Conference (ICRC2023)
26 July - 3 August, 2023
Nagoya, Japan

*Speaker

PoS(ICRC2023)190

1. Introduction

Cosmic rays (CRs) are one of the most important components in the interstellar medium, mainly consisting of protons (hydrogen nuclei)[1]. Due to the small flux of cosmic rays with energy above 10^{14} eV, indirect measurements are required by using ground detectors[2]. When a primary cosmic ray goes through atmosphere, it will undergo hadronic or electromagnetic interaction[3] and then produce a massive number of secondary particles that are scattered over an area of several square kilometers, known as an Extensive Air Shower (EAS)[4]. For some ground-based experiments, the altitude dependence of the showers was one of the first characteristics studied by numerous researchers. Within decades, a large number of measurements had been carried out from sea level to high altitude mountain areas[5]. LHAASO, a cosmic ray detection instrument[6], is well suited to study the unique EAS phenomenon, due to its location at Mount Haizi in Daocheng County, Sichuan Province, China, at an altitude of 4410 m.

The impact of thunderstorms on the development of EAS is one of the hot topics in high-energy atmospheric physics. As common meteorological events, thunderstorms bring heavy rainstorms, strong winds, and lightning flashes[7]. The maximum strength of electric fields could be up to 1000 V/cm[8] or even 2000 V/cm[9, 10] during thunderstorms. In such strong fields, by accelerating/decelerating or deflecting the charged particles in EAS, the properties of the secondary cosmic rays are affected. Therefore, many scientists have studied the changes in secondary cosmic rays during thunderstorms.

In 1985, the intensity variations of ground cosmic rays during thunderstorms were first demonstrated by Alexeenko et al.[11]. And the thunderstorm ground enhancements (TGEs) have been proposed in 2010[12]. Subsequently, Zhou et al.[13] simulated the effects of electric fields on the variations of the secondary cosmic ray intensity, which were found to be highly dependent on the strength and polarity of the electric field. In addition, the energy variations of secondary particles were analyzed and the energy spectrum was softened in the presence of the field[14]. So far, numerous simulation studies of the variations of cosmic rays caused by an AEF have been done to obtain a clearer images.

For ground-based experiments (e.g., LHAASO, ARGO-YBJ), the information on the arrival time and location of each particle is recorded to reconstruct the shower core position, the primary energy, and arrival direction. During thunderstorms, the trajectories of secondary particles from EAS could be modified, leading to changes of the shower rate[15, 16, 17].

In this work, the CORSIKA code is used to simulate the EAS development, and the G4KM2A code is used to simulate the response of LHAASO-KM2A detector. With a vertical and uniform AEF model, the effects of near-earth electric fields on the cosmic ray shower rates recorded by LHAASO-KM2A are simulated.

2. Simulation parameters

CORSIKA is a detailed simulation program for extensive air showers initiated by high energy cosmic particles. In this work, the CORSIKA software package (version 77410) is used to simulate air showers in the atmosphere. The hadronic interaction models are QGSJETII-04 in the high energy range (>80 GeV) and GHEISHA for low energy events (< 80 GeV). Since protons predominate in

the cosmic rays, the simulated primary particles are selected as protons. According to the energy threshold of the LHAASO-KM2A detector, the primary energy of protons are ranging from 1 to 10^5 TeV following a power-law function with a spectral index of -2.7. We assume proton primaries with arrival directions uniformly distributed in the sky, with a zenith angle in the interval from 0 to 60°. Considering the acceleration of the electric field, the secondary positrons, electrons and photons are tracked until their energies decreased to 50 keV.

During a thunderstorm, the strength and polarity of the electric field change significantly. According to the theory proposed by Symbalisty et al.[18] and Dwyer[19], the field strength threshold ($E_{\rm th}$) to trigger the RREA process can be calculated. At LHAASO site (4410 m), $E_{\rm th}$ is about 1660 V/cm. At the altitude of 6210 m, $E_{\rm th}$ is about 1336 V/cm. To study the AEF effects, a simple model with vertical and uniform atmospheric electric field is used, and the field ranges from -1600 to 1600 V/cm in this work. Due to the atmospheric attenuation, the effects on the secondary particles can be neglected in electric field, which is far from detectors[20]. In our simulations, the AEF is applied in a layer of atmosphere extending from the detector level (4410 m) up to 6210 m.

As the largest component of LHAASO, the whole KM2A array (as shown in Fig. 1) is composed of 5216 electromagnetic particle detectors (EDs) and 1188 muon detectors (MDs), and started running stably from 20 July 2021.

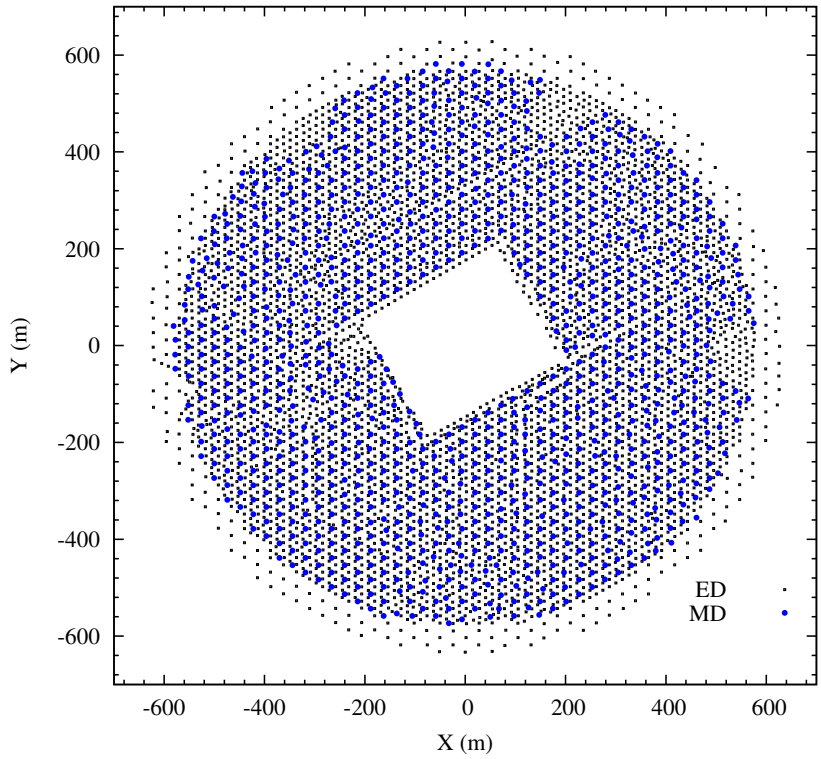

Fig. 1. Layout of the whole KM2A array. The black diamonds and blue dots indicate the EDs and MDs, respectively.

To simulate the response of the KM2A detector, a specific software, G4KM2A[21], is developed in the framework of the GEANT4 software package[22]. When the trigger conditions are satisfied (at least 20 EDs are fired within a time window of 400 ns, as in the observations), the shower event

is recorded. In order to be more similar to the LHAASO-KM2A experiment, the background rate per ED is set to 1700 Hz[23], and the radius of the sample area is 1000 m.

3. Simulation results

Previous studies have shown that the intensity variations of secondary particles are dependent on the AEF strength and the thicknesses of the AEF layer[13, 16]. To understand the change of shower data detected by ground-based experiments(e.g., LHAASO-KM2A), the EAS development and detector response are simulated with different parameters for the AEF model.

3.1 The AEF strength dependence of the shower rate variations

To study the correlation between the shower rate variation and the AEF strength, the typical AEF layer thickness of AEF layer 1000 m (extending from the detector altitude of 4410 m up to 5410 m) is used. Fig. 2(a) and Fig. 2(b) show the percent variation of the triggered shower rate recorded by the whole KM2A array in negative and positive electric fields, respectively. It can be seen that the total shower rate increases during a thunderstorm, and the amplitude increases quickly with the field intensity, especially for a field magnitude larger than 1400 V/cm. The enhanced amplitude is about 17% in a field of -1200 V/cm and the value could be up to 46% when the electric field reaches -1600 V/cm. From Fig. 2, we can see that the increased amplitude is larger in negative AEF. In a field of -1000 V/cm, the rate of shower events is enhanced by up to 12%, and merely reach 6% in a positive one with the same field strength.

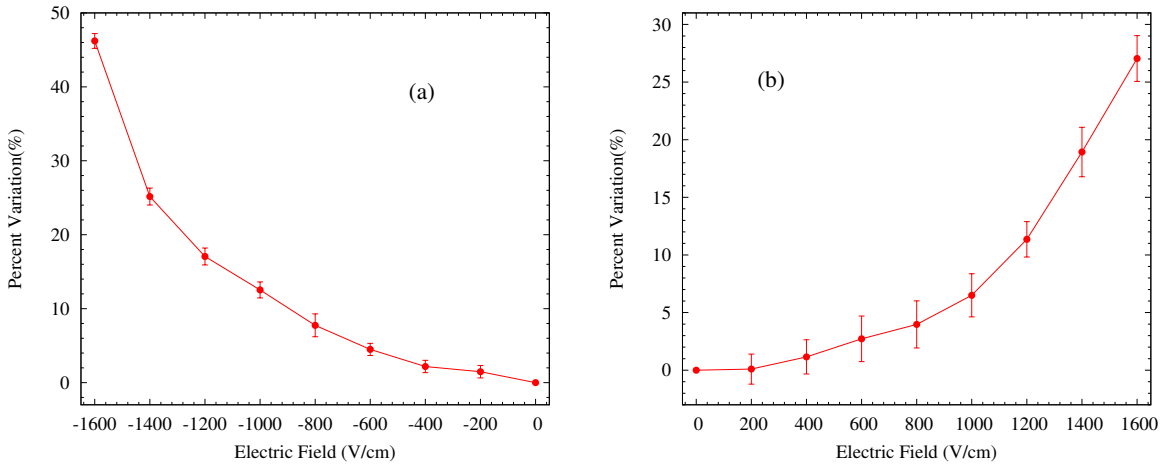

Fig. 2. Percent variations of the total shower rate as a function of the electric field intensity, assuming the AEF layer of thickness 1000 m. (a): in negative field, (b): in positive field.

Therefore, we infer that the intensity variations of shower events recorded by LHAASO-KM2A are highly dependent on the strength and the polarity of thunderstorm fields.

3.2 The AEF layer thickness dependence of the shower rate variations

The results in Fig. 2 have been obtained by assuming the thickness of the AEF layer to be 1000 m. Fig. 3 shows the variations of shower rate as a function of the vertical field length in the atmosphere above the detector, assuming AEF intensity of ±1000 V/cm. It can be seen that the trigger event rate increases dramatically at small thickness, and the increasing in amplitude in a negative field is larger than in a positive one. When the thickness of the AEF layer is 1200 m, the variation in magnitude is up to 14% in a negative field, while it only reaches 8% in a positive one. If the thickness is higher than 1200 m, the curve flattens out in a positive or negative field. The variation trends are in good qualitative agreement with the previous paper [16]. We believe that the the AEF at higher altitudes has a small influence on the development of an EAS. Alternatively, for large thicknesses of the AEF layer, the deflection effect on charged particles may be more significant than the acceleration effect.

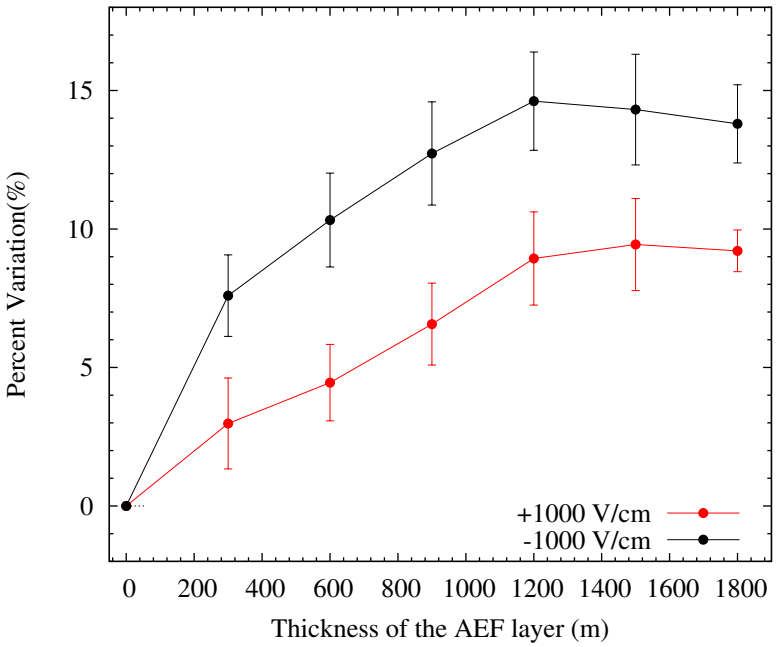

Fig. 3. The total shower rate variations as a function of the thickness of AEF layer in ±1000 V/cm.

From Fig. 2 and Fig. 3, we can see that shower rate variations are related to the AEF strength and the thickness of the AEF layer. To get more information, Fig. 4 shows the variations as a function of AEF layer thickness with fields of -800 V/cm, -1000 V/cm, and -1500 V/cm. We can see that shower rates increase and the variations become larger with the increasing field intensities. When the thickness is 300 m, the variation amplitude reaches 4% in -800 V/cm, 7% in -1000 V/cm, and 15% in -1500 V/cm. With the increasing thickness of AEF layer, there is no flattening trend in the curve of -1500 V/cm up to 1800 m. However, the other two curves flatten at the thicknesses of $\sim$ 900 m in -800 V/cm, and $\sim$ 1200 m in -1000 V/cm.

Fig. 5 shows the variations in positive fields. It can be seen that the variations are consistent with the results in negative fields, but the amplitude are smaller.

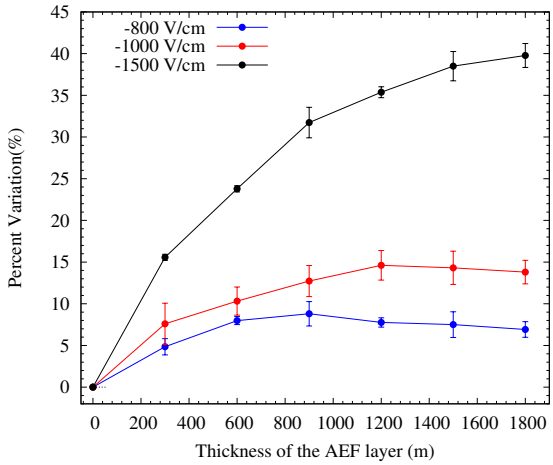

Fig. 4. The total shower rate variation as a function of the thickness of AEF layer in negative fields.

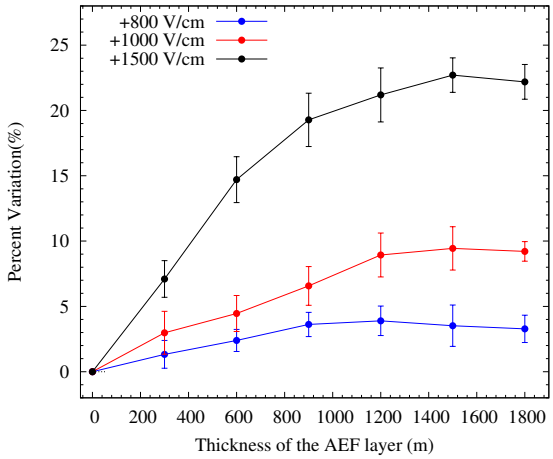

Fig. 5. The total shower rate variation as a function of the thickness of AEF layer in positive fields.

3.3 The zenith angle dependence of the shower rate variations

It is well known that the atmospheric depth increases with the zenith angle[24]. Thus, the field effects on the shower events should be associated with primary cosmic ray directions[25]. Fig. 6 shows the variations of shower rate as a function of zenith angle in the field strength of 1000 V/cm, assuming an AEF layer of thickness 1500 m. We can see that the shower rate is enhanced for smaller zenith angle ranges, but is reduced for higher zenith angle ranges. The variation trends are in good qualitative agreement with the results in our previous paper[16]. At the same time, the variation amplitude is related to the field polarity. For zenith angle θ= 25°, the values of enhancements are 7% in +1000 V/cm and 14% in -1000 V/cm.

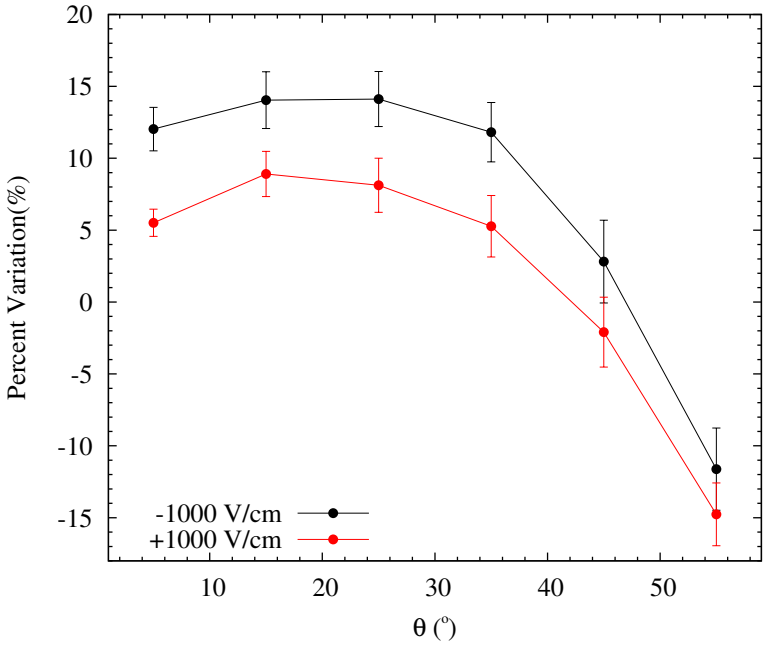

Fig. 6. Percent variations of the shower event rate as a function of the zenith angle, assuming the AEF layer of thickness 1500 m.

4. Summary

In this paper, Monte Carlo simulations are used to study the effects of near-earth thunderstorm electric fields on cosmic ray showers recorded by LHAASO-KM2A. Significant shower rate variations are observed in correlation with the AEF strength. The variation amplitude increases with the field intensity. With the same field strength, the increased amplitude is larger in a negative field. Meanwhile, the variations also depend on the thickness of the AEF layer. The trigger rate increases rapidly at small thickness, and when the thickness of the AEF layer reaches a certain value (depending on the electric field), the curve starts to flatten out.

In addition, the variation of shower rate is related to the primary zenith angle. We find that the shower rate is enhanced for smaller zenith angles, but is reduced for higher ones both in positive and negative electric fields. These results are consistent with our previous simulation results[16], and be helpful in understanding the variation of shower detection rate in LHAASO-KM2A during thunderstorms.

Acknowledgments

This work is supported by the National Natural Science Foundation of China (NSFC) under the Grant No. U2031101, and the National Key R&D Program of China under the grant No.2018YFA0404201. The authors would like to express their sincere thanks to the members of the LHAASO collaboration.

References

[1] R. Z. Yang, University of Science and Technology of China, **53**(1), 2 (2023).
[2] M. Zha et al., Chinese Journal of Nature, **34**(2), 80 - 82 (2012).
[3] B. Xu et al., Journal of Southwest Jiaotong University (English Edition), **03**, 290–294 (2008).
[4] Z. C. Huang et al., Acta. Physica. Sinica., **70**, 199301 (2021).
[5] K. F. Grieder Peter, Springer-Verlag Berlin Heidelberg, **1**, 6 (2010).
[6] http://www.chinadaily.com.cn/a/202210/20/WS635146a5a310fd2b29e7da62.html, retrieved 12 June 2023
[7] X. S. Qie et al., Science China Earth Sciences, **64**(1), 10-26 (2021).
[8] T. C. Marshall et al., J. Geophys. Res., **100**, 1001–1015 (1995).
[9] M. Stolzenburg et al., Geophys. Res. Lett., **34**, L04804 (2007).
[10] T. C. Marshall et al., Geophys. Res. Lett., **32**, L03813 (2005).
[11] Alexeenko et al., 19th ICRC, **5**, 352 (1985).
[12] A. Chilingarian et al., Phys. Rev. D, **82**, 043009 (2010).
[13] X. X. Zhou et al., Astropart. Phys., **84**, 107 (2016).
[14] R. R. Yan et al., Chin. Astron. Astr., **44**(2), 146-159 (2020).
[15] K. G. Axi et al. (ARGO-YBJ Collaboration), Phys. Rev. D, **106**, 022008 (2022).
[16] F. Aharonian et al. (LHAASO Collaboration), Chin. Phys. C, **47**, 015001 (2023).
[17] S. Vernetto for EAS-TOP Collaboration. 27th ICRC, **10**, 4165 (2001).
[18] E. M. D. Symbalisty et al., Plasma Sci. **26**, 1575 (1998).
[19] J. R. Dwyer, Geophys. Res. Lett., **30**(20), 2055 (2003).
[20] X. X. Zhou et al., Chin. J. Space Sci. **36**(1), 49-55 (2016).
[21] https://pos.sissa.it/358/219/pdf, retrieved 12 June 2023
[22] S. Agostinelli et al. (GEANT4 collaboration), Nucl. Instrum. Meth. A, **506**, 250 (2003).
[23] F. Aharonian et al., Nucl. Instrum. Meth. A, **1001**, 165193 (2021).
[24] K. G. Axi et al. Astrophys. Space Sci., **367**, 30 (2022).
[25] S. Buitink et al., Astropart. Phys., **33**(1), 1–12 (2010).

Full Authors List: LHAASO Collaboration

Zhen Cao[1,2,3], F. Aharonian[4,5], Q. An[6,7], Axikegu[8], Y.X. Bai[1,3], Y.W. Bao[9], D. Bastieri[10], X.J. Bi[1,2,3], Y.J. Bi[1,3], J.T. Cai[10], Q. Cao[11], W.Y. Cao[7], Zhe Cao[6,7], J. Chang[12], J.F. Chang[1,3,6], A.M. Chen[13], E.S. Chen[1,2,3], Liang Chen[14], Lin Chen[8], Long Chen[8], M.J. Chen[1,3], M.L. Chen[1,3,6], Q.H. Chen[8], S.H. Chen[1,2,3], S.Z. Chen[1,3], T.L. Chen[15], Y. Chen[9], N. Cheng[1,3], Y.D. Cheng[1,3], M.Y. Cui[12], S.W. Cui[11], X.H. Cui[16], Y.D. Cui[17], B.Z. Dai[18], H.L. Dai[1,3,6], Z.G. Dai[7], Danzengluobu[15], D. della Volpe[19], X.Q. Dong[1,2,3], K.K. Duan[12], J.H. Fan[10], Y.Z. Fan[12], J. Fang[18], K. Fang[1,3], C.F. Feng[20], L. Feng[12], S.H. Feng[1,3], X.T. Feng[20], Y.L. Feng[15], S. Gabici[21], B. Gao[1,3], C.D. Gao[20], L.Q. Gao[1,2,3], Q. Gao[15], W. Gao[1,3], W.K. Gao[1,2,3], M.M. Ge[18], L.S. Geng[1,3], G. Giacinti[13], G.H. Gong[22], Q.B. Gou[1,3], M.H. Gu[1,3,6], F.L. Guo[14], X.L. Guo[8], Y.Q. Guo[1,3], Y.Y. Guo[12], Y.A. Han[23], H.H. He[1,2,3], H.N. He[12], J.Y. He[12], X.B. He[17], Y. He[8], M. Heller[19], Y.K. Hor[17], B.W. Hou[1,2,3], C. Hou[1,3], X. Hou[24], H.B. Hu[1,2,3], Q. Hu[7,12], S.C. Hu[1,2,3], D.H. Huang[8], T.Q. Huang[1,3], W.J. Huang[17], X.T. Huang[20], X.Y. Huang[12], Y. Huang[1,2,3], Z.C. Huang[8], X.L. Ji[1,3,6], H.Y. Jia[8], K. Jia[20], K. Jiang[6,7], X.W. Jiang[1,3], Z.J. Jiang[18], M. Jin[8], M.M. Kang[25], T. Ke[1,3], D. Kuleshov[26], K. Kurinov[26], B.B. Li[11], Cheng Li[6,7], Cong Li[1,3], D. Li[1,2,3], F. Li[1,3,6], H.B. Li[1,3], H.C. Li[1,3], H.Y. Li[7,12], J. Li[7,12], Jian Li[7], Jie Li[1,3,6], K. Li[1,3], W.L. Li[20], W.L. Li[13], X.R. Li[1,3], Xin Li[6,7], Y.Z. Li[1,2,3], Zhe Li[1,3], Zhuo Li[27], E.W. Liang[28], Y.F. Liang[28], S.J. Lin[17], B. Liu[7], C. Liu[1,3], D. Liu[20], H. Liu[8], H.D. Liu[23], J. Liu[1,3], J.L. Liu[1,3], J.Y. Liu[1,3], M.Y. Liu[15], R.Y. Liu[9], S.M. Liu[8], W. Liu[1,3], Y. Liu[10], Y.N. Liu[22], R. Lu[18], Q. Luo[17], H.K. Lv[1,3], B.Q. Ma[27], L.L. Ma[1,3], X.H. Ma[1,3], J.R. Mao[24], Z. Min[1,3], W. Mitthumsiri[29], H.J. Mu[23], Y.C. Nan[1,3], A. Neronov[21], Z.W. Ou[17], B.Y. Pang[8], P. Pattarakijwanich[29], Z.Y. Pei[10], M.Y. Qi[1,3], Y.Q. Qi[11], B.Q. Qiao[1,3], J.J. Qin[7], D. Ruffolo[29], A. Sáiz[29], D. Semikoz[21], C.Y. Shao[17], L. Shao[11], O. Shchegolev[26,30], X.D. Sheng[1,3], F.W. Shu[31], H.C. Song[27], Yu.V. Stenkin[26,30], V. Stepanov[26], Y. Su[12], Q.N. Sun[8], X.N. Sun[28], Z.B. Sun[32], P.H.T. Tam[17], Q.W. Tang[31], Z.B. Tang[6,7], W.W. Tian[2,16], C. Wang[32], C.B. Wang[8], G.W. Wang[7], H.G. Wang[10], H.H. Wang[17], J.C. Wang[24], K. Wang[9], L.P. Wang[20], L.Y. Wang[1,3], P.H. Wang[8], R. Wang[20], W. Wang[17], X.G. Wang[28], X.Y. Wang[9], Y. Wang[8], Y.D. Wang[1,3], Y.J. Wang[1,3], Z.H. Wang[25], Z.X. Wang[18], Zhen Wang[13], Zheng Wang[1,3,6], D.M. Wei[12], J.J. Wei[12], Y.J. Wei[1,2,3], T. Wen[18], C.Y. Wu[1,3], H.R. Wu[1,3], S. Wu[1,3], X.F. Wu[12], Y.S. Wu[7], S.Q. Xi[1,3], J. Xia[7,12], J.J. Xia[8], G.M. Xiang[2,14], D.X. Xiao[11], G. Xiao[1,3], G.G. Xin[1,3], Y.L. Xin[8], Y. Xing[14], Z. Xiong[1,2,3], D.L. Xu[13], R.F. Xu[1,2,3], R.X. Xu[27], W.L. Xu[25], L. Xue[20], D.H. Yan[18], J.Z. Yan[12], T. Yan[1,3], C.W. Yang[25], F. Yang[11], F.F. Yang[1,3,6], H.W. Yang[17], J.Y. Yang[17], L.L. Yang[17], M.J. Yang[1,3], R.Z. Yang[7], S.B. Yang[18], Y.H. Yao[25], Z.G. Yao[1,3], Y.M. Ye[22], L.Q. Yin[1,3], N. Yin[20], X.H. You[1,3], Z.Y. You[1,3], Y.H. Yu[7], Q. Yuan[12], H. Yue[1,2,3], H.D. Zeng[12], T.X. Zeng[1,3,6], W. Zeng[18], M. Zha[1,3], B.B. Zhang[9], F. Zhang[8], H.M. Zhang[9], H.Y. Zhang[1,3], J.L. Zhang[16], L.X. Zhang[10], Li Zhang[18], P.F. Zhang[18], P.P. Zhang[7,12], R. Zhang[7,12], S.B. Zhang[2,16], S.R. Zhang[11], S.S. Zhang[1,3], X. Zhang[9], X.P. Zhang[1,3], Y.F. Zhang[8], Yi Zhang[1,12], Yong Zhang[1,3], B. Zhao[8], J. Zhao[1,3], L. Zhao[6,7], L.Z. Zhao[11], S.P. Zhao[12,20], F. Zheng[32], B. Zhou[1,3], H. Zhou[13], J.N. Zhou[14], M. Zhou[31], P. Zhou[9], R. Zhou[25], X.X. Zhou[8], C.G. Zhu[20], F.R. Zhu[8], H. Zhu[16], K.J. Zhu[1,2,3,6], X. Zuo[1,3], (The LHAASO Collaboration)

[1] Key Laboratory of Particle Astrophyics & Experimental Physics Division & Computing Center, Institute of High Energy Physics, Chinese Academy of Sciences, 100049 Beijing, China

[2] University of Chinese Academy of Sciences, 100049 Beijing, China

[3] TIANFU Cosmic Ray Research Center, Chengdu, Sichuan, China

[4] Dublin Institute for Advanced Studies, 31 Fitzwilliam Place, 2 Dublin, Ireland

[5] Max-Planck-Institut for Nuclear Physics, P.O. Box 103980, 69029 Heidelberg, Germany

[6] State Key Laboratory of Particle Detection and Electronics, China

[7] University of Science and Technology of China, 230026 Hefei, Anhui, China

[8] School of Physical Science and Technology & School of Information Science and Technology, Southwest Jiaotong University, 610031 Chengdu, Sichuan, China

[9] School of Astronomy and Space Science, Nanjing University, 210023 Nanjing, Jiangsu, China

[10] Center for Astrophysics, Guangzhou University, 510006 Guangzhou, Guangdong, China

[11] Hebei Normal University, 050024 Shijiazhuang, Hebei, China

[12] Key Laboratory of Dark Matter and Space Astronomy & Key Laboratory of Radio Astronomy, Purple Mountain Observatory, Chinese Academy of Sciences, 210023 Nanjing, Jiangsu, China

[13] Tsung-Dao Lee Institute & School of Physics and Astronomy, Shanghai Jiao Tong University, 200240 Shanghai, China

[14] Key Laboratory for Research in Galaxies and Cosmology, Shanghai Astronomical Observatory, Chinese Academy of Sciences, 200030 Shanghai, China

PoS(ICRC2023)190

[15] Key Laboratory of Cosmic Rays (Tibet University), Ministry of Education, 850000 Lhasa, Tibet, China

[16] National Astronomical Observatories, Chinese Academy of Sciences, 100101 Beijing, China

[17] School of Physics and Astronomy (Zhuhai) & School of Physics (Guangzhou) & Sino-French Institute of Nuclear Engineering and Technology (Zhuhai), Sun Yat-sen University, 519000 Zhuhai & 510275 Guangzhou, Guangdong, China

[18] School of Physics and Astronomy, Yunnan University, 650091 Kunming, Yunnan, China

[19] Département de Physique Nucléaire et Corpusculaire, Faculté de Sciences, Université de Genève, 24 Quai Ernest Ansermet, 1211 Geneva, Switzerland

[20] Institute of Frontier and Interdisciplinary Science, Shandong University, 266237 Qingdao, Shandong, China

[21] APC, Université Paris Cité, CNRS/IN2P3, CEA/IRFU, Observatoire de Paris, 119 75205 Paris, France

[22] Department of Engineering Physics, Tsinghua University, 100084 Beijing, China

[23] School of Physics and Microelectronics, Zhengzhou University, 450001 Zhengzhou, Henan, China

[24] Yunnan Observatories, Chinese Academy of Sciences, 650216 Kunming, Yunnan, China

[25] College of Physics, Sichuan University, 610065 Chengdu, Sichuan, China

[26] Institute for Nuclear Research of Russian Academy of Sciences, 117312 Moscow, Russia

[27] School of Physics, Peking University, 100871 Beijing, China

[28] School of Physical Science and Technology, Guangxi University, 530004 Nanning, Guangxi, China

[29] Department of Physics, Faculty of Science, Mahidol University, Bangkok 10400, Thailand

[30] Moscow Institute of Physics and Technology, 141700 Moscow, Russia

[31] Center for Relativistic Astrophysics and High Energy Physics, School of Physics and Materials Science & Institute of Space Science and Technology, Nanchang University, 330031 Nanchang, Jiangxi, China

[32] National Space Science Center, Chinese Academy of Sciences, 100190 Beijing, China

PoS(ICRC2023)190